

Control of a quasi-one-dimensional phase of a Si nanostructure: Vicinal Si(557) surfacesM. K. Kim,^{1,2} D.-H. Oh,^{1,*} J. Baik,³ C. Jeon,^{1,2} I. Song,¹ J. H. Nam,¹ S. H. Woo,⁴ C.-Y. Park,^{1,2,5,†} and J. R. Ahn^{1,2,6,‡}¹*BK21 Physics Research Division, Sungkyunkwan University, 300 Cheoncheon-dong, Jangan-gu, Suwon 440-746, Korea*²*Center for Nanotubes and Nanostructured Composites (CNNC), Sungkyunkwan University, 300 Cheoncheon-dong, Jangan-gu, Suwon 440-746, Korea*³*Beamline Research Division, Pohang Accelerator Laboratory, Pohang, 790-784 Kyungbuk, Korea*⁴*College of Pharmacy, Chungnam National University, Daejeon 305-764, Republic of Korea*⁵*Department of Energy Science, Sungkyunkwan University, 300 Cheoncheon-dong, Jangan-gu, Suwon 440-746, Korea*⁶*SKKU Advanced Institute of Technology (SAINT), Sungkyunkwan University, 300 Cheoncheon-dong, Jangan-gu, Suwon 440-746, Korea*

(Received 12 January 2010; published 8 February 2010)

The quasi-one-dimensional phase of a Si nanostructure was tuned in a controllable manner by changing the crystallographic orientation and thermal treatment conditions and was observed by scanning tunneling microscopy. A small change in the crystallographic orientation of a Si(557) surface stabilized the quasi-one-dimensional 5×5 phase and made it coexist with a quasi-one-dimensional 7×7 phase after an optimal thermal treatment, whereas only the quasi-one-dimensional 7×7 phase was stable on the Si(557) surface. Interestingly, this causes the (111) terraces with finite widths to prefer only one of the 5×5 and 7×7 phases resulting in long-range order of both the 5×5 and 7×7 phases along the step edge direction, which was supported by first-principles calculations. In contrast, the quasi-one-dimensional 5×5 and 7×7 phases were arranged randomly across the step edge direction.

DOI: [10.1103/PhysRevB.81.085312](https://doi.org/10.1103/PhysRevB.81.085312)

PACS number(s): 68.35.bg, 68.35.Rh, 68.37.Ef

I. INTRODUCTION

A nanotemplate is an essential framework in a bottom-up approach to the fabrication of functional nanomaterials.¹ A wide range of nanostructures on reconstructed metal and semiconductor surfaces have resulted in an abundance of the low-dimensional functional nanomaterials. The unique structures of Si surfaces have been used to produce interesting nanoclusters and nanowires which are different from ones on metal surfaces.²⁻¹² Various metal atoms have been reported to form magic nanoclusters with the same size as the unit cell of the Si(111)- 7×7 surface.²⁻⁶ The selective reactions of metal atoms on the Si(111)- 7×7 surface with faulted and unfaulted unit cells resulted in a well-ordered two-dimensional array of magic nanoclusters.^{2,3,6} Vicinal Si(111) surfaces have mainly been considered for the fabrications of nanowires based on nanotemplates. In particular, the interesting phenomena of Au-induced nanowires on Si(557) and Si(553) surfaces had boosted researches into nanowire fabrications on vicinal Si(111) surfaces.^{10,13-15} The exotic electronic and electric properties of Pb nanowires on the Si(553) surface highlight the importance of the vicinal Si(111) surfaces as nanotemplates.¹⁶

A reconstructed Si(557) surface is unique among the vicinal Si(111) surfaces because it has a well-ordered reconstructed surface with an alternative order of (111) and (112) terraces with finite widths, where the (111) terrace undergoes the same surface reconstruction as the Si(111)- 7×7 surface.¹⁷ The few nm scale width of the (111) and (112) terrace on the Si(557) surface could be a promising nanotemplate for functional materials such as a quasi-one-dimensional (1D) array of magic nanoclusters on the (111) terraces. In this study, the coexistence of the quasi-1D 5×5 and 7×7 phases was achieved on a vicinal Si(557) surface by controlling its crystalline orientation. Rapid ther-

mal quenching was not used in the thermal treatment, whereas a disordered 1×1 phase of a high-temperature Si(111) surface shows the coexistence of two-dimensional 5×5 and 7×7 phases at room temperature (RT) only after rapid thermal quenching.¹⁸ The coexistence of the quasi-1D phases was optimized by adjusting the annealing time at 1100 K and were stable over a wide temperature range of 1088 K to RT, which were visualized directly by scanning tunneling microscopy (STM), as shown in Fig. 1. The coexistence of the quasi-1D phases is explained successfully in terms of the relative stability of the 5×5 and 7×7 phases on a (111) terrace with a finite width, which was calculated by first-principles calculations. The T_c s resulting from the relative stability of the two phases were consistent with the STM experiments. The control of the quasi-1D phase on the vicinal Si(557) surface can provide a different framework in the fabrications of functional nanomaterials on the Si(557) surface.

II. EXPERIMENTS AND CALCULATIONS

The STM images were acquired using a commercial VT-STM (Omicron) at RT. Three types of *n*-type (P-doped) vicinal Si(111) wafers with resistivity of $1 \Omega \text{ cm}$ were used. One was a Si(557) wafer with an off-angle of 9.45° from the (111) surface toward the $[\bar{1}\bar{1}2]$ direction and the others were vicinal Si(557) wafers with off-angles of 0.3° and 0.6° , respectively, from the (557) surface toward the $[11\bar{2}]$ direction. The off angles of the wafers were measured by x-ray diffraction accurately with an error of $\pm 0.01^\circ$. Clean surfaces were prepared by repeated resistive heating, where an electric voltage was applied along the step edge direction to prepare a uniform step edge structure.¹⁷ Pseudopotential numerical atomic orbital calculations were carried out based on the

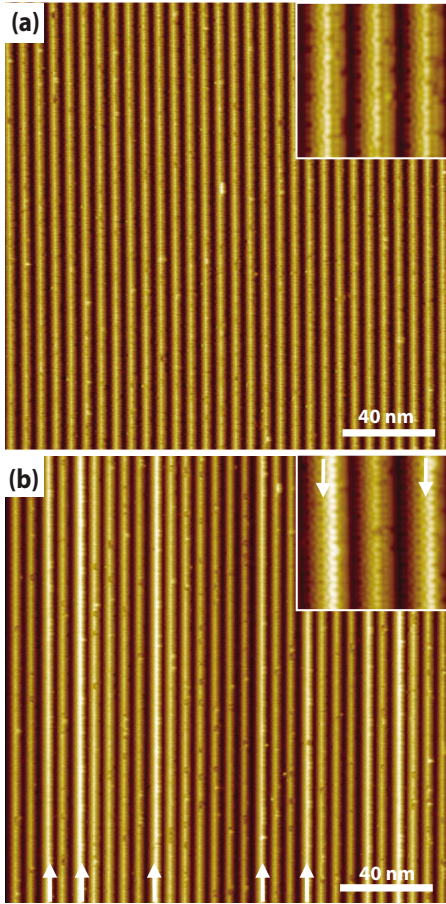


FIG. 1. (Color online) The empty-state STM images of (a) the Si(557) surface with $\alpha=0^\circ$ and (b) the vicinal Si(557) surface with $\alpha=0.6^\circ$, where the insets are the enlarged images and the arrows indicate the quasi-1D 5×5 phases.

density-functional theory within the local-density approximation using SIESTA code.¹⁹ In the calculations, norm-conserving pseudopotentials in the Kleinman-Bylander form and double-zeta basis sets were used. Atomic structure models were based on three Si bilayers, where the bottom Si atoms were saturated by H atoms.

III. RESULTS AND DISCUSSIONS

Figure 2(a) shows the empty-state STM image of a Si(557) surface. The Si(557) surface was prepared using the following thermal treatment. After flashing at 1520 K, the sample was cooled to 1320 K for 30 s and was quenched to 1100 K within 2 s. The sample was finally cooled to RT for 2 min after annealing for 30 min at 1100 K.¹⁷ A reconstructed Si(557) surface consists of one (111) terrace with atomic rows (L) of 9 and three (112) terraces with $L=2\frac{2}{3}$, as shown in Fig. 2(b). The (111) terrace undergoes the same surface reconstruction as the Si(111)- 7×7 surface,¹⁷ as shown in Fig. 2(a). Figures 2(c)–2(e) show empty-state STM images of the vicinal Si(557) surfaces. The same thermal treatment used for the Si(557) surface was applied except for the annealing time (t_a) at 1100 K. t_a was critical in controlling the

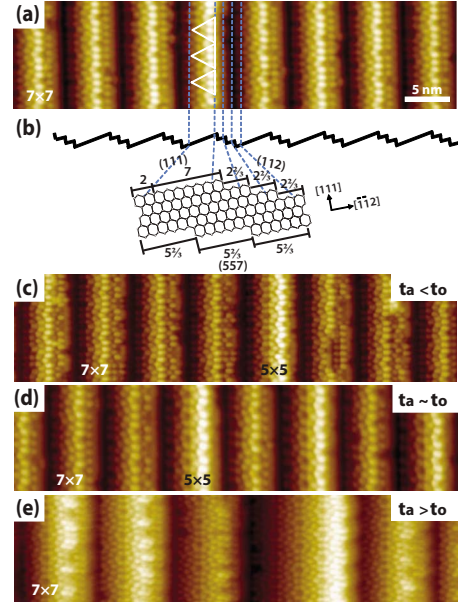


FIG. 2. (Color online) (a) The empty-state STM image and (b) bulk-terminated atomic structure of the Si(557) surface, where the triangles denote the half unit cell of the 7×7 phase. The empty-state STM images of a vicinal Si(557) surface with $\alpha=0.6^\circ$ when the annealing time (t_a) at 1100 K was (c) 5, (d) 30, and (e) 420 min, respectively. t_o is the optimal t_a for the quasi-1D phase coexistence of the 5×5 and 7×7 phases.

overall structure of the vicinal Si(557) surface. When t_a was less than 5 min, the step edge structures were not uniform and there were many atomic defects [see Fig. 2(c)]. The atomic defects were caused by a lack of atomic migration, where the atomic migration was induced by an electric current.²⁰ Most defects at the step edges were cured at $t_a > 30$ min., as shown in Fig. 2(d). A quasi-1D 5×5 phase was found to coexist with a quasi-1D 7×7 phase after curing the sample for $30 \text{ min} < t_a < 90 \text{ min}$. When $t_a > 400$ min, the widths of the (111) terraces were widened further. This widening resulted in the disappearance of the (111) terraces with the quasi-1D 5×5 phases. This was accompanied by the creation of (111) terraces which have quasi-1D 7×7 phases with more than a half unit cell of the 7×7 phase across the step edge direction, as shown in Fig. 2(e).²¹

The coexistence of the quasi-1D 5×5 and 7×7 phases were further studied by controlling the off-angle (α) from the Si(557) surface toward the $[11\bar{2}]$ direction. Figure 3 shows surface reconstructions on vicinal Si(557) surfaces with increasing α . Figure 3(a) shows the empty-state STM image of the Si(557) surface with $\alpha=0^\circ$. The Si(557) surface is built up of one (111) terrace with $L=9$ and three (112) terraces with $L=2\frac{2}{3}$, as described above, where the (111) terrace undergoes the same surface reconstruction as the Si(111)- 7×7 surface.¹⁷ With increasing α , the 7×7 phase began to coexist with the 5×5 phase, as shown in Fig. 3(b). The widths of the quasi-1D 5×5 and 7×7 domains were $L=12$ and $L=9$, respectively, which are close to the single unit cell of the 5×5 phase and the half unit cell of the 7×7 phase on a Si(111) surface, respectively [see Figs.

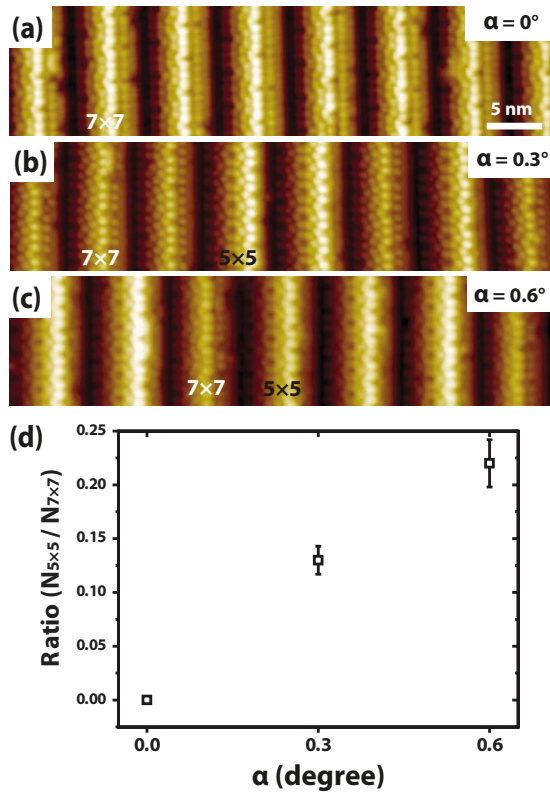


FIG. 3. (Color online) The empty-state STM images of (a) the Si(557) surface with $\alpha=0^\circ$ and the vicinal Si(557) surfaces with (b) $\alpha=0.3^\circ$ and (c) 0.6° . The ratio of the 5×5 phase to the 7×7 phase is shown in (d).

3(a)–3(c)]. Interestingly, either the 5×5 or 7×7 phases were found on a single (111) terrace without the coexistence of the two phases. More interestingly, the correlation lengths of both the 5×5 and 7×7 phases along the step edge direction were above 200 nm, as shown in Fig. 1. In contrast, the quasi-1D 5×5 and 7×7 phases were arranged randomly across the step edge direction. The ratio of the number of the quasi-1D 5×5 phases to the number of the quasi-1D 7×7 phases increased with increasing α , as shown in Fig. 3(d). The stability of the quasi-1D 5×5 phase was examined by long-time postannealing at a temperature below 1100 K, where the 5×5 phase is optimized at 1100 K. Figure 4 shows the dependence of the vicinal Si(557) surfaces on the postannealing temperature (T) and time (t_a). First, coexisting quasi-1D 5×5 and 7×7 phases were prepared through the optimized thermal process described above. Second, the Si surfaces were postannealed at a temperature below 1100 K. The STM images of the vicinal Si(557) surfaces in Fig. 4 were measured at RT after the postannealing. The quasi-1D 5×5 phase was still observed even after the long-time postannealing. Moreover, the ratio of the quasi-1D 5×5 and 7×7 phases was invariant. This suggests that the coexisting quasi-1D 5×5 and 7×7 phases are stable over a wide temperature range of RT to 1088 K.

In general, the surface total energy of a vicinal surface is a function of two principle factors, the surface tension related to faceting and a surface reconstruction on a terrace.²² STM images showed that the change in the surface tension due to

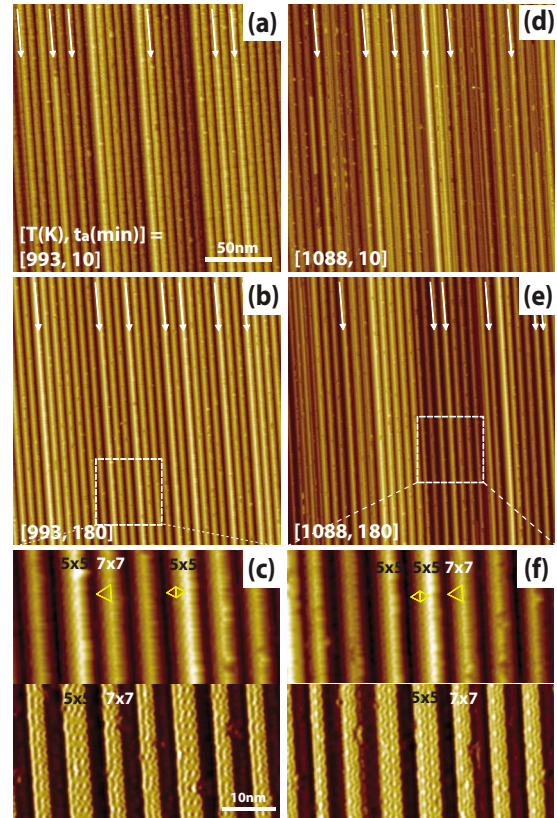


FIG. 4. (Color online) [(a)–(f)] The empty-state STM images of the vicinal Si(557) surface with $\alpha=0.6^\circ$. The STM images show the dependence of the vicinal Si(557) surface on the annealing temperature (T) and time (t_a). The upper images in (c) and (f) are the enlarged images of (b) and (e), respectively. The lower images in (c) and (f) are the derivatives of the enlarged images used to clarify the widths of the (111) terraces. The arrows and triangles indicate the quasi-1D 5×5 phases and the unit cells of the 5×5 and 7×7 phases, respectively.

α modifies only the ratio of the two types of (111) terraces with different atomic rows, where the distribution of the two types of (111) terraces across the step edge direction was random, as shown in Fig. 1(b). Furthermore, the (111) terrace with $L=9$ produced only the 7×7 phase, while the (111) terrace with $L=12$ showed only the 5×5 phase. The coexistence of the quasi-1D 5×5 and 7×7 phases is thus a matter of energetic selection between the two phases on a given (111) terrace width.

The relative stability of the 5×5 phase to the 7×7 phase on the (111) terraces with finite widths was calculated by using first-principles calculations. The 5×5 and 7×7 phases on the (111) terraces have the same atomic structures as the dimer-atom-stacking (DAS) fault models of the Si(111)- 5×5 and Si(111)- 7×7 phases, respectively.²³ In the calculations, only the (111) terraces were considered without the (112) terraces because surface reconstructions on the (112) terraces do not depend on the arrangement of the 5×5 and 7×7 phases and the whole unit cell is too large to be calculated. Four atomic structure models, 7×7 and 5×5 structures on the two types of (111) terraces with $L=9$ and $L=12$, respectively, were testified, as shown in Fig.

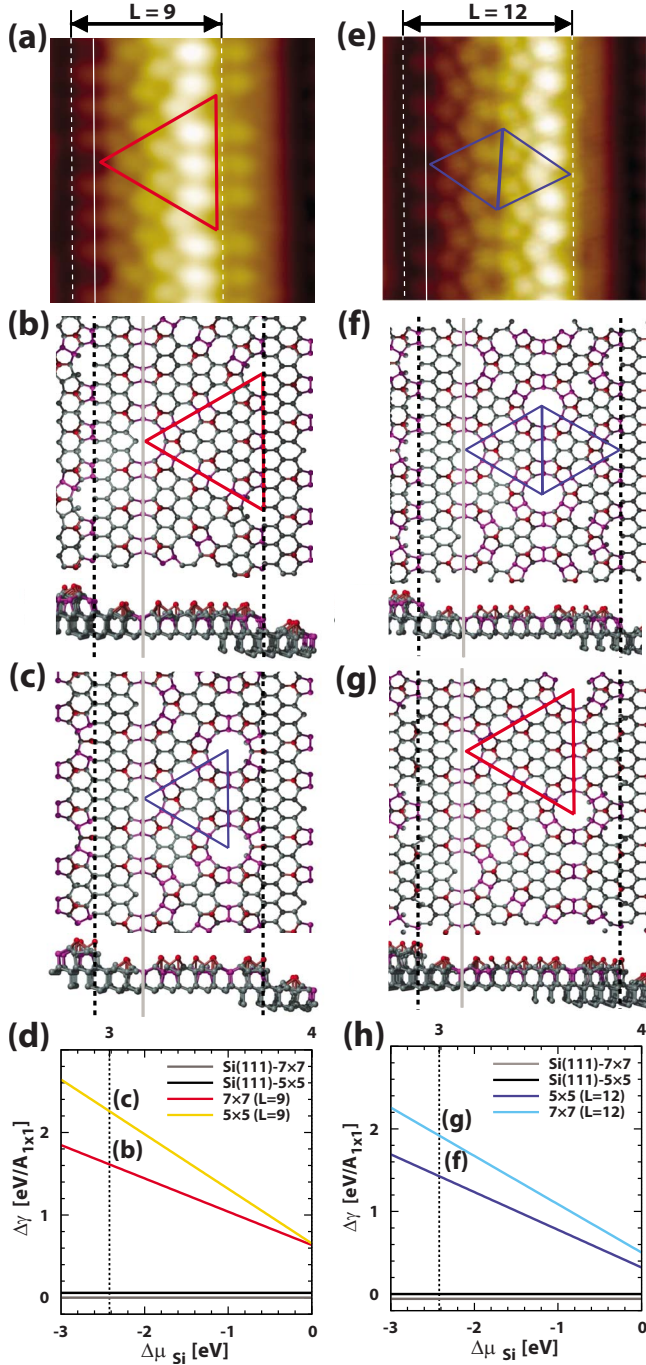


FIG. 5. (Color online) The empty-state STM images of (a) the 7×7 and (e) 5×5 phases. The atomic structure models of (b) the 7×7 and (c) 5×5 phases on the (111) terrace with $L=9$ and (f) the 5×5 and (g) 7×7 phases on the (111) terrace with $L=12$. Here, the solid triangles indicate their unit cell and the dotted and solid lines indicate the (111) terraces and the boundaries between the buffer region and 7×7 (or 5×5) phase, respectively. The γ of the two phases on the (111) terraces with (d) $L=9$ and (h) $L=12$ as a function of $\Delta\mu_{\text{Si}}$.

5. A buffer region with $L=2$ is located between the step edge and 7×7 (or 5×5) structure, as shown in the STM images. Figures 5(b), 5(c), 5(f), and 5(g) show the atomic structure of

the buffer region, which was reported on vicinal Si(111) surfaces.^{24,25}

The surface free energy γ of the atomic structure is $E_{\text{tot}} - n_{\text{Si}}\mu_{\text{Si}}^{\text{bulk}} - n_{\text{H}}\mu_{\text{H}} - n_{\text{Si}}\Delta\mu_{\text{Si}}$,²⁶ where E_{tot} is the total energy per unit area calculated by first-principles calculations, $\mu_{\text{Si}}(\mu_{\text{H}})$ is the chemical potential of a Si (H) atom, the μ of a bulk Si atom $\mu_{\text{Si}}^{\text{bulk}}$ is $\mu_{\text{Si}} - \Delta\mu_{\text{Si}}$, and $n_{\text{Si}}(n_{\text{H}})$ is the number of Si (H) atoms per unit area. The uppermost Si atoms have different μ s from $\mu_{\text{Si}}^{\text{bulk}}$, while the underlying Si atoms have similar μ s to $\mu_{\text{Si}}^{\text{bulk}}$. Then, γ is replaced by $E_{\text{total}} - n_{\text{Si}}\mu_{\text{Si}}^{\text{bulk}} - n_{\text{H}}\mu_{\text{H}} - n_{\text{Si}}^{\text{S}}\Delta\mu_{\text{Si}}$, where n_{Si}^{S} is the number of Si atoms at the uppermost bilayer. In the atomic structures, half of Si atoms in the uppermost bilayer are threefold coordinated and the remainder are fourfold coordinated. A meaningful $\Delta\mu_{\text{Si}}$ is thus near -1.2 eV and at least below -0.6 eV because the $\Delta\mu_{\text{Si}}$ s of a bulk Si atom and a Si atom with a single dangling bond are 0 and -2.4 eV, respectively. Therefore, the 7×7 (5×5) phase on the (111) terrace with $L=9$ ($L=12$) is at least 174 (258) meV more energetically stable than the 5×5 (7×7) phase, as shown in Figs. 5(d) and 5(h), where the relative $\gamma(\Delta\gamma)$ to the γ of the 7×7 phase on a Si(111) surface is used for convenience in Figs. 5(d) and 5(h). The relative instability at the given (111) terrace is because the DAS-like structure is not terminated at its unit-cell boundary at the step edge and consequently leaves many Si dangling bonds at the step edge with increasing γ . This suggests that the DAS-like structures on (111) terraces prefer to be terminated at their unit-cell boundary in order to minimize Si dangling bonds, as observed on other vicinal Si(111) surfaces.^{21,27} The differences in γ suggest that the T_c of the 7×7 (5×5) phase on the (111) terrace with $L=9$ ($L=12$) is above 2088 (3092) K. The T_c s indicate that the coexisting quasi-1D phases are robust below 2000 K when the surface is not destroyed by an external effect such as surface melting. This is consistent with the fact that the coexisting quasi-1D phases are stable until the terrace widths are changed significantly through an order-disorder transition between the 7×7 (or 5×5) and 1×1 phases with a T_c of 1123 K.²²

The surface reconstructions on the vicinal Si(557) surfaces are required to satisfy their overall crystallographic orientations. In the case of a Si(557) surface, a combination of one (111) terrace with $L=9$ and three (112) terraces with $L=2\frac{2}{3}$ matches the overall (557) orientation [see Fig. 6(a)].^{17,28} When a vicinal Si(557) surface is tilted slightly from the (557) surface, the number of atomic rows of (111) terraces needs to be adjusted in order to satisfy the overall orientation of a vicinal Si(557) surface. There are many combinations of (111) terraces with different atomic rows matching the overall orientation of a vicinal Si(557) surface. STM images suggest that, in principle, there is no order across the step edge direction of (111) terraces with different atomic rows. Here, the ordered cases of (111) terraces are described for convenience. When a regular step array of the vicinal Si(557) surface is produced from only one type of a (111) terrace, as shown in Fig. 6(b), one (111) terrace with $L=12$ and three (112) terraces with $L=2\frac{2}{3}$ can satisfy the overall orientation of $\alpha=1.4^\circ$. When two types of (111) terraces are used as building blocks, two (111) terraces with $L=9$ and $L=12$, respectively, and three (112) terraces with $L=2\frac{2}{3}$ can

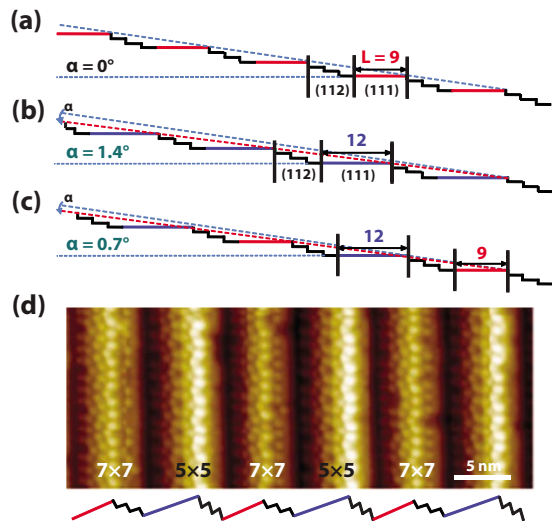


FIG. 6. (Color online) The schematic diagrams of the arrangements of (111) and (112) terraces across the step edge direction for (a) the Si(557) surface and [(b)–(c)] the vicinal Si(557) surfaces. The blue and red lines denote the (111) terraces with $L=12$ and $L=9$, respectively. (d) The empty-state STM image of the vicinal Si(557) surface with $\alpha=0.6^\circ$.

be matched with the overall orientation of $\alpha=0.7^\circ$, as shown in Fig. 6(c). Figure 6(d) shows the alternative arrangement of 5×5 and 7×7 phases across the step edge direction, which was rarely observed because there is no order across the step

edge direction. This supports that the coexistence of the quasi-1D 5×5 and 7×7 phases can occur, when α is between 0° and 1.4° .

IV. CONCLUSIONS

The coexistence of the quasi-1D 5×5 and 7×7 phases was observed directly by STM. The quasi-1D phase coexistence was achieved by tilting the Si(557) surface slightly toward the $[11\bar{2}]$ direction. The off angles from the (557) surface produced two types of (111) terraces with different atomic rows. The (111) terraces with $L=9$ and $L=12$ underwent the same surface reconstructions as the 5×5 and 7×7 phases on a Si(111) surface, respectively. These phases were stabilized energetically by terminating their unit-cell boundaries at the step edges, which was supported by first-principles calculations. The 7×7 (5×5) phase on the (111) terrace with $L=9$ ($L=12$) was approximately 174 (258) meV more energetically stable than the 5×5 (7×7) phase.

ACKNOWLEDGMENTS

This work was supported by the Korea Science and Engineering Foundation (KOSEF) grant funded by the Korea government (MEST) (Grant No. 2009-0080512) and Priority Research Centers Program through the National Research Foundation of Korea (NRF) (Grant No. 20090094026) and World Class University (WCU) program (Grant No. R31-2008-000-10029-0).

*ohdh@skku.edu

†cypark@skku.edu

‡jrahn@skku.edu

- ¹J. V. Barth, G. Costantini, and K. Kern, *Nature (London)* **437**, 671 (2005).
- ²J. L. Li, J. F. Jia, X. J. Liang, X. Liu, J. Z. Wang, Q. K. Xue, Z. Q. Li, J. S. Tse, Z. Zhang, and S. B. Zhang, *Phys. Rev. Lett.* **88**, 066101 (2002).
- ³S. C. Li, J. F. Jia, R. F. Dou, Q. K. Xue, I. G. Batyrev, and S. B. Zhang, *Phys. Rev. Lett.* **93**, 116103 (2004).
- ⁴V. G. Kotlyar, A. V. Zotov, A. A. Saranin, T. V. Kasyanova, M. A. Cherevik, I. V. Pisarenko, and V. G. Lifshits, *Phys. Rev. B* **66**, 165401 (2002).
- ⁵H. Wang and Z. Q. Zoua, *Appl. Phys. Lett.* **88**, 103115 (2006).
- ⁶J. H. Byun, J. R. Ahn, W. H. Choi, P. G. Kang, and H. W. Yeom, *Phys. Rev. B* **78**, 205314 (2008).
- ⁷I. Barke, R. Bennowitz, J. N. Crain, S. C. Erwin, A. Kirakosian, J. L. McChesney, and F. J. Himpsel, *Solid State Commun.* **142**, 617 (2007).
- ⁸J. R. Ahn, J. H. Byun, H. Koh, E. Rotenberg, S. D. Kevan, and H. W. Yeom, *Phys. Rev. Lett.* **93**, 106401 (2004).
- ⁹J. N. Crain, J. L. McChesney, F. Zheng, M. C. Gallagher, P. C. Snijders, M. Bissen, C. Gundelach, S. C. Erwin, and F. J. Himpsel, *Phys. Rev. B* **69**, 125401 (2004).
- ¹⁰P. C. Snijders, S. Rogge, and H. H. Weitering, *Phys. Rev. Lett.* **96**, 076801 (2006).

- ¹¹H. S. Yoon, S. J. Park, J. E. Lee, C. N. Whang, and I. W. Lyo, *Phys. Rev. Lett.* **92**, 096801 (2004).
- ¹²I. Song, D.-H. Oh, J. H. Nam, M. K. Kim, C. Jeon, C.-Y. Park, S. H. Woo, and J. R. Ahn, *New J. Phys.* **11**, 063034 (2009).
- ¹³R. Losio, K. N. Altmann, A. Kirakosian, J.-L. Lin, D. Y. Petrovykh, and F. J. Himpsel, *Phys. Rev. Lett.* **86**, 4632 (2001).
- ¹⁴J. R. Ahn, H. W. Yeom, H. S. Yoon, and I.-W. Lyo, *Phys. Rev. Lett.* **91**, 196403 (2003).
- ¹⁵J. R. Ahn, P. G. Kang, K. D. Ryang, and H. W. Yeom, *Phys. Rev. Lett.* **95**, 196402 (2005).
- ¹⁶K. S. Kim and H. W. Yeom, *Nano Lett.* **9**, 1916 (2009).
- ¹⁷A. Kirakosian, R. Bennowitz, J. N. Crain, Th. Fauster, J.-L. Lin, D. Y. Petrovykh, and F. J. Himpsel, *Appl. Phys. Lett.* **79**, 1608 (2001).
- ¹⁸R. S. Becker, J. A. Golovchenko, G. S. Higashi, and B. S. Swartzentruber, *Phys. Rev. Lett.* **57**, 1020 (1986); K. Takayanagi, Y. Tanishiro, and K. Kajiyama, *J. Vac. Sci. Technol. B* **4**, 1074 (1986); R. M. Feenstra and M. A. Lutz, *ibid.* **9**, 716 (1991).
- ¹⁹J. M. Soler, E. Artacho, J. D. Gale, A. García, J. Junquera, P. Ordejón, and D. Sánchez-Portal, *J. Phys.: Condens. Matter* **14**, 2745 (2002).
- ²⁰S. Yoshida, T. Sekiguchi, and K. M. Itoha, *Appl. Phys. Lett.* **87**, 031903 (2005).
- ²¹J. L. Goldberg, X.-S. Wang, J. Wei, N. C. Bartelt, and E. D. Williams, *J. Vac. Sci. Technol. A* **9**, 1868 (1991).

- ²²F. K. Men, F. Liu, P. J. Wang, C. H. Chen, D. L. Cheng, J. L. Lin, and F. J. Himpsel, *Phys. Rev. Lett.* **88**, 096105 (2002).
- ²³K. Takayanagi, Y. Tanishiro, M. Takahashi, and S. Takahashi, *J. Vac. Sci. Technol. A* **3**, 1502 (1985).
- ²⁴D.-H. Oh, M. K. Kim, J. H. Nam, I. Song, C.-Y. Park, S. H. Woo, H.-N. Hwang, C. C. Hwang, and J. R. Ahn, *Phys. Rev. B* **77**, 155430 (2008).
- ²⁵T. Sekiguchi, S. Yoshida, and K. M. Itoh, *Phys. Rev. Lett.* **95**, 106101 (2005).
- ²⁶A. A. Stekolnikov, J. Furthmüller, and F. Bechstedt, *Phys. Rev. B* **65**, 115318 (2002).
- ²⁷R. S. Becker, J. A. Golovchenko, E. G. McRae, and B. S. Swartzentruber, *Phys. Rev. Lett.* **55**, 2028 (1985).
- ²⁸K. S. Kim, W. H. Choi, and H. W. Yeom, *Phys. Rev. B* **75**, 195324 (2007).